

# Cesium Fountain Primary Frequency Standard NMIJ-F2 with Uncertainty Evaluated

Akifumi Takamizawa, Shinya Yanagimachi, and Ken Hagimoto

National Metrology Institute of Japan  
National Institute of Advanced Industrial Science and Technology (AIST)  
1-1-1 Umezono, Tsukuba, Ibaraki 305-8563, Japan

**Summary**—We completed the first uncertainty evaluation of NMIJ-F2, the second cesium fountain primary frequency standard at National Metrology Institute of Japan. The type A uncertainty was given as  $2.3 \times 10^{-13}(\tau/s)^{-1/2}$  ( $\tau$ : averaging time), and the total type B uncertainty was  $4.6 \times 10^{-16}$ . In addition, we started contribution to the calibration of International Atomic Time. The frequency of NMIJ-F2 agreed well with that of the other primary and secondary frequency standards within the uncertainty.

**Keywords**—cesium fountain; primary frequency standard; uncertainty evaluation; International Atomic Time

## I. INTRODUCTION

Atomic fountains have realized the unit of seconds defined by the transition frequency of cesium atoms the most accurately [1]. At National Metrology Institute of Japan (NMIJ), we have developed cesium fountain primary frequency standards (PFSs) [2-5]. Recently, we completed the first uncertainty evaluation of our second cesium fountain, NMIJ-F2 [5], and started contribution to the calibration of International Atomic Time (TAI) for the first time since our first fountain, NMIJ-F1 [2], was stopped in 2011 due to the huge earthquake. Moreover, NMIJ-F2 compared with the Yb optical lattice clock, NMIJ-Yb1, to search scalar dark matter [6].

NMIJ-F2 has the features: (1) the microwave cavities which are part of the vacuum vessel [7], (2) The high atom number by high laser power (around 50 mW per cooling beam) and optical pumping to  $m_F = 0$  [3,8], which is the Zeeman sublevel used in Ramsey interrogation for frequency measurements, (3) the cryocooled sapphire oscillator (cryoCSO) as a local oscillator with a frequency stability of  $3 \times 10^{-15}$  at 1 s [9], and (4) the external cavity diode lasers (ECDLs) with a highly reliable frequency lock [10, 11]. The feature (1) reduces the uncertainty due to microwave leakage. The features (2) and (3) improve the frequency stability. Then, the feature (4) contributes to long-term operation; the numbers of unintentional mode hops in the two ECDLs were 1 for the one and 0 for the other in 5 months.

Table I shows the uncertainty budget of NMIJ-F2 in the report to Bureau International des Poids et Mesures (BIPM) during MJD 59819 – MJD 59849. The total type B uncertainty was  $4.6 \times 10^{-16}$ . The uncertainties of a distributed cavity phase (DCP) shift and a microwave leakage shift were dominant. The budget was modified on the blackbody radiation and gravity from the first uncertainty evaluation.

In this presentation, we report the uncertainty evaluation of NMIJ-F2, focusing on a collisional shift, a DCP, and microwave leakage. Moreover, we describe contribution to TAI via reports to BIPM. Compared to ref. [5], which describes the details of the uncertainty evaluation, this proceeding includes some updates of the frequency stability and frequency comparison with the primary and secondary frequency standards (PSFSs). Moreover, the unpublished figure showing the density distributions after state-selection is added.

TABLE I. Uncertainty budget of NMIJ-F2. The correction for a collisional shift is for low density.

Effect	Correction/ $10^{-16}$	Uncertainty/ $10^{-16}$
Second-order Zeeman	−1725.6	0.6
Blackbody radiation	+167.5	0.7
Collisional shift	+28.0	0.3
Distributed cavity phase	0	3.4
Lensing	0	0.9
Microwave leakage	−1.2	2.5
Background gas pressure	0	1.0
Gravity	−16.8	0.1
Light shift	0	< 0.01
Rabi, Ramsey pulling	0	0.4
Cavity pulling	0	0.9
Spurious	0	0.2
Total	−1548.1	4.6

## II. RESULTS

### A. Collisional shift and frequency stability

A collisional shift is proportional to the density of atoms. The frequency at zero density is extrapolated from the frequencies at high and low densities with the ratio  $\kappa = 4$  during frequency measurement. Therefore, the type A uncertainty includes the uncertainty of a collisional shift. Figure 1 shows the overlapping Allan deviations as a function of averaging

time  $\tau$ . At high density, the frequency stability was obtained as  $7.0 \times 10^{-14}(\tau/s)^{-1/2}$ . Due to the extrapolation, the frequency stability at zero density was degraded to  $2.3 \times 10^{-13}(\tau/s)^{-1/2}$ . Nevertheless, it was good enough because the type A uncertainty reached  $1.7 \times 10^{-16}$  at  $\tau = 20$  d.

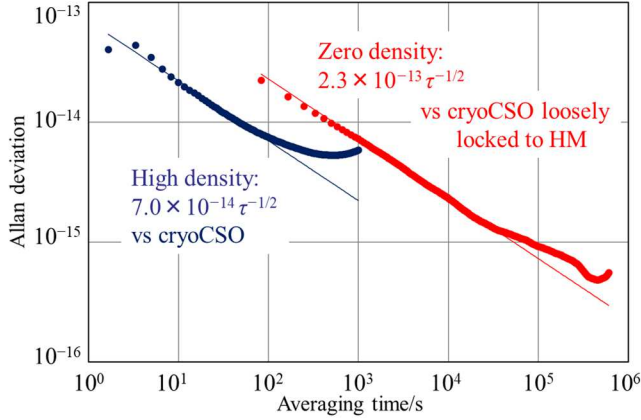


Fig. 1. Overlapping Allan deviations of frequency at high density (blue) and zero density (red). Here, the reference oscillator was a cryoCSO for high density and a cryoCSO locked to a hydrogen maser (HM) at a time constant of 100 s for zero density.

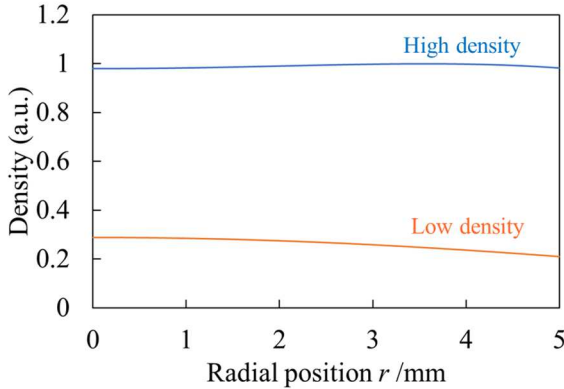


Fig. 2. Calculated density distributions at high density (blue) and low density (orange) as a function of a radial position in the state-selection cavity.

The atom number is alternated by changing the amplitude of a state-selection microwave pulse, not using the adiabatic passage method [12]. The amplitude distribution of the microwave in the state-selection cavity is expressed by a Bessel function and thus inhomogeneous. Moreover, the transition probability is represented by a sinusoidal function on interaction time with a period proportional to microwave amplitude. These make the difference between the density distributions of atoms at high and low densities and may induce the non-linearity between frequency and the atom number, leading to the type B uncertainty.

To evaluate it, the density distributions just after the state selection were calculated, assuming that the initial distribution was homogenous. The calculation result at high and low densities as a function of a radial position are shown in Fig. 2.

The difference between the density distributions at high and low densities was calculated to be very small. Estimating collisional shifts from the density distributions, averaging them over the aperture of the cavity with a radius of 5 mm, and taking the ratio of the averaged collisional shifts between high and low densities as  $\kappa_c$ , the frequency shift due to nonlinearity is given by

$$\Delta f_{c(nl)} = \left( \frac{\kappa_c - 1}{\kappa_c + 1} \right) \cdot \Delta f_{c(L)}. \quad (1)$$

Here,  $\Delta f_{c(L)}$  is the collisional shift at a low density. Consequently, it is derived that  $\Delta f_{c(nl)} = 0.011 \Delta f_{c(L)}$  and typically  $3 \times 10^{-17}$ . We take it as a type B uncertainty.

### B. Distributed cavity phase

When the phase of the microwave in the Ramsey cavity is Fourier-expanded with  $\cos(m\phi)$  ( $m \geq 0$ , integer), the components at  $m = 0, 1$ , and  $2$  are need to be considered. We experimentally evaluated the uncertainty of the DCP shift ( $m = 1$ ) to be  $1.3 \times 10^{-16}$  in the feed direction of the microwave and  $1.6 \times 10^{-16}$  in the perpendicular direction. The uncertainty evaluation of the former was done by the following steps similarly with ref. [13]: (1) the alignment of the vertical cooling laser beams with reflection from water surface, (2) the Ramsey microwave was fed from only one side, and the frequency was measured as a function of the fountain tilt. The frequency measurements with feed from the other side were also performed. The fountain tilt at which their frequency difference was zero was found. (3) the amplitude and phase of the Ramsey microwave to the two opposing feeds were balanced and adjusted, respectively. Then, the tilt dependence of the frequency was measured. (4) the fountain tilt was adjusted to the zero cross in (2) as close as possible. Then, the uncertainty for the DCP shift was evaluated from the deviation of the tilt from the zero cross and tilt dependence of the frequency.

As for  $m = 0$  and  $2$ , we conservatively estimated the upper limits, taking the calculation result from ref. [14] under somewhat different conditions; the inner diameter of the cavity is 47 mm for ours and 52 mm for the reference. The uncertainties of the DCP shifts ( $m = 0$  and  $2$ ) were evaluated as  $1.0 \times 10^{-16}$  and  $2.5 \times 10^{-16}$ , respectively.

### C. Microwave leakage

Because the feedthroughs of the microwave cavity are attached outside the vacuum chamber, microwave leakage from the feedthroughs is negligible for interrogated atoms. However, leakage from the central aperture of the cavity may induce a frequency shift because the Ramsey microwave is continuously on. To suppress it, a frequency shift key in a direct digital synthesizer is used to detune the microwave frequency by 100 kHz after atoms pass through the Ramsey cavity. The microwave leakage shift was evaluated by measuring the frequency of the fountain at pulse areas of the Ramsey microwave,  $n_p\pi/2$  ( $n_p = 1, 3, 5, 7$ ), and fitting the curve  $\Delta f_{lk} = A n_p \sin(n_p\pi/2)$ , where  $A$  is a constant [15]. The frequency was measured for 5 d per pulse area, and TAI was used as reference. As a result, it was obtained that  $A = (+1.2 \pm 2.5) \times 10^{-16}$ , which corresponded to the frequency shift and its uncertainty at  $\pi/2$  pulses.

#### D. Updates from the first uncertainty evaluation

The uncertainty of the blackbody radiation shift was slightly improved from  $0.9 \times 10^{-16}$  to  $0.7 \times 10^{-16}$  by replacing the coefficient  $\beta$  between temperature and blackbody radiation shift given in [16] with the one given in [17]. For the gravity, while the gravitational potential of the mean sea level of Tokyo Bay was used at the first evaluation, the gravitational potential of NMIJ-Yb1, which is located in the same building, was more precisely evaluated by geophysical experts very recently [18]. By using the latter, the uncertainty of the gravitational shift was reduced from  $0.6 \times 10^{-16}$  to  $0.1 \times 10^{-16}$ .

#### E. Frequency data reported to BIPM

Figure 3 shows the fractional frequency difference between NMIJ-F2 and PSFSs,  $y(\text{NMIJF2} - \text{PSFS})$ , for the data reported to BIPM. Here, the blue dots and red squares represents the cases where the values were reported after and before the publication of the circular T, respectively. There were 13 reports including 2 on-time reports over approximately 3 years. The weighted mean of  $y(\text{NMIJF2} - \text{PSFS})$  was  $-1.5 \times 10^{-15}$ , and the chi-square test statics was  $\chi^2/\nu = 0.32$ . These indicates the frequency of NMIJ-F2 agreed well with that of PSFSs within the uncertainty.

Currently, NMIJ-F2 works well. However, because the hydrogen maser whose frequency was measured by the fountain was rapidly degraded very recently, we replaced it with another one in January 2023. After the replacement, we have confirmed agreement between NMIJ-F2 and PSFSs via circular T without reporting. We will restart reports of frequency data to BIPM soon.

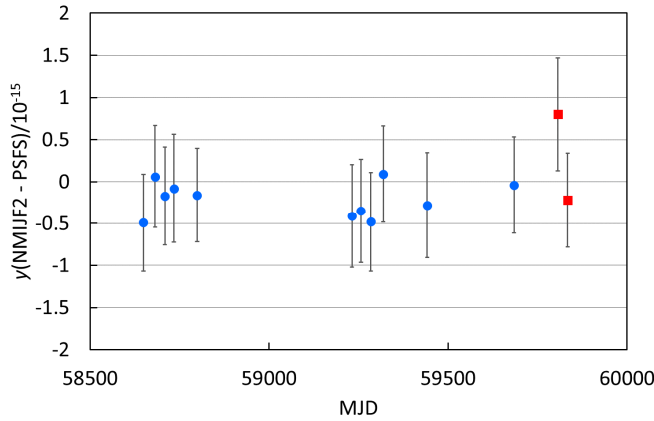


Figure 3.  $y(\text{NMIJF2} - \text{PSFS})$  for the data reported to BIPM.

### III. CONCLUSIONS

We believe that the current uncertainty of NMIJ-F2 is so small that the fountain can highly contribute to calibration of TAI. Therefore, we will conduct long-term frequency measurement for reports to BIPM (approximately one month per report) in priority to reduction of the uncertainty for a few years.

As a next step for reduction of the uncertainty, the calculation of the DCP shift ( $m = 0, 2$ ) under the condition of NMIJ-F2 may be effective. Moreover, the use of an interference switch [19] for evaluation of the microwave leakage may reduce

the uncertainty. After these efforts, the total type B uncertainty is expected to be reduced by a factor of 2.

#### ACKNOWLEDGMENT

This work was supported by JSPS KAKENHI Grant Numbers JP 22H01241, 18K04989 and 15K21669.

#### REFERENCES

- [1] R. Wynands and S. Weyers, "Atomic fountain clocks," *Metrologia*, vol. 42, no. 3, pp. S64-S79, 2005.
- [2] T. Kurosu, Y. Fukuyama, Y. Koga, and K. Abe, "Preliminary evaluation of the Cs atomic fountain frequency standard at NMIJ/AIST," *IEEE Trans. Instrum. Meas.*, vol. 53, no. 2, pp. 466-471, 2004.
- [3] A. Takamizawa, S. Yanagimachi, T. Tanabe, K. Hagimoto, I. Hirano, K. Watabe, T. Ikegami, and J. G. Hartnett, "Atomic fountain clock with very high frequency stability employing a pulse-tube-cryocooled sapphire oscillator," *IEEE Trans. Ultrason. Ferroelectr. Freq. Control*, vol. 61, no. 9, pp. 1463-1469, 2014.
- [4] A. Takamizawa, S. Yanagimachi, T. Tanabe, K. Hagimoto, I. Hirano, K. Watabe, T. Ikegami, and J. G. Hartnett, "Preliminary Evaluation of the Cesium Fountain Primary Frequency Standard NMIJ-F2," *IEEE Trans. Instrum. Meas.*, vol. 64, no. 9, pp. 2504-2512, 2015.
- [5] A. Takamizawa, S. Yanagimachi, and K. Hagimoto, "First uncertainty evaluation of the cesium fountain primary frequency standard NMIJ-F2," *Metrologia*, vol. 59, no. 3, art. No. 035004, 2022.
- [6] T. Kobayashi et al., "Search for Ultralight Dark Matter from Long-Term Frequency Comparisons of Optical and Microwave Atomic Clocks," *Phys. Rev. Lett.* vol. 129, no. 24, art. No. 241301, 2022.
- [7] S. R. Jefferts et al. R. E. Drullinger, and A. DeMarchi, "NIST cesium fountain microwave cavities," in *Proc. IEEE Freq. Control Symp.*, May 1998, pp. 6-8.
- [8] K. Szymaniec, H.-R. Noh, S. E. Park, and A. Takamizawa, "Spin polarization in a freely evolving sample of cold atoms," *Appl. Phys. B*, vol. 111, no. 3, pp. 527-535, 2013.
- [9] J. G. Hartnett, N. R. Nand, and C. Lu, "Ultra-low-phase-noise cryocooled microwave dielectric-sapphire-resonator oscillators," *Appl. Phys. Lett.*, vol. 100, no. 18, art. No. 183501, 2012.
- [10] A. Takamizawa, S. Yanagimachi, T. Ikegami, and R. Kawabata, "External cavity diode laser with frequency drift following natural variation in air pressure," *Appl. Opt.*, vol. 54, no. 18, pp. 5777-5781, 2015.
- [11] A. Takamizawa, S. Yanagimachi, and T. Ikegami, "External cavity diode laser with very-low frequency drift," *Appl. Phys. Express*, vol. 9, no. 3, Art. No. 032704, 2016.
- [12] F. Pereira Dos Santos, H. Marion, S. Bize, Y. Sortais, A. Clairon, and C. Salomon, "Controlling the Cold Collision Shift in High Precision Atomic Interferometry," *Phys. Rev. Lett.* vol. 89, no. 23, art. No. 233004, 2002.
- [13] J. Guéna, J., R. Li, K. Gibble, S. Bize, and A. Clairon, "Evaluation of Doppler Shifts to Improve the Accuracy of Primary Atomic Fountain Clocks," *Phys. Rev. Lett.*, vol. 106, no. 13, art. no. 130801, 2011.
- [14] R. Li, and K. Gibble, "Evaluating and minimizing distributed cavity phase errors in atomic clocks," *Metrologia*, vol. 47, no. 5, pp. 534-551, 2010.
- [15] T. P. Heavner et al., "First Accuracy Evaluation of NIST-F2," *Metrologia*, vol. 51, no. 3, pp. 174-182, 2014.
- [16] K. Beloy, U. I. Safronova, and A. Derevianko, "High-Accuracy Calculation of the Blackbody Radiation Shift in the  $^{133}\text{Cs}$  Primary Frequency Standard," *Phys. Rev. Lett.* vol. 97, no. 4, art. No. 040801, 2006.
- [17] P. Rosenbusch, S. Zhang, and A. Clairon, "Blackbody radiation shift in primary frequency standards," 2007 *Proc. European Frequency and Time Forum*, pp. 1060-1063, 2007.
- [18] M. Nakashima, S. Fukaya, T. Toyofuku, K. Ochi, and K. Matsuo, "Determination of geopotential values at the optical lattice clocks based on geodetic approaches," 2022 *Proc. Japan Geoscience Union Meeting*, SGD02-14, 2022.

- [19] G. Santarelli, et al., "Switching atomic fountain clock microwave interrogation signal and high-resolution phase measurements," IEEE Trans. Ultrason. Ferroelectr. Freq. Control, vol. 56, no. 7, pp. 1319-1326, 2009.